Microstructure morphological optimization of foam-based lightweight insulators

M T Hoang, Camille Perrot, V. Marcel, J.-F Rondeau

Microstructure morphological optimization of foam-based lightweight insulators

M. T. Hoang[1], C. Perrot[2], V. Marcel[1], J.-F. Rondeau[1]

1: Faurecia Acoustics and Soft Trim Division, Acoustic TechCenter, Z.I. François Sommer BP 13, 08210 Mouzon, France

2: Université Paris-Est, Laboratoire Modélisation et Simulation Multi Echelle, MSME UMR 8208 CNRS, 5 bd Descartes, 77454 Marne-la-Vallée, France

Abstract: This paper presents a new optimization method of the acoustic behavior of poroelastic polyurethane (PUR) foams. Using the Finite Transfer Matrix Method, a set of optimal Biot parameters is determined for optimized possible insulation or absorption properties of specialized foams: airflow resistivity, tortuosity, Young's modulus, etc. Following a chemically controllable microstructure morphology change such as cell size or membrane closure rate, a space of admissible microstructures is found. The 3D hybrid numerical approach developed by Hoang and Perrot, based on three necessary input parameters, is used to link the foam local geometry to its acoustical macro-behavior. Hence, an optimized cell morphology space is identified reaching macro-acoustic targets for absorption purposes such as the first layer of a Light-Weight Concept system or for insulation purposes such as the foam spring of any multi-layer insulator. This optimization procedure allows to go beyond classical schemes and gives a high potential for weight reduction or acoustic performance improvement for foam-based insulators.

Keywords: Optimization, microstructure, absorption, insulation, PUR foams

1. Introduction

For many years the weight reduction in cars has been a key issue in order to reduce energy consumption and pollution, driven by the new upcoming CO2 emission regulations (limited to 95 g CO2/km in 2020). Since the acoustic package for noise treatment presents a significant percentage of the car's total weight, this requirement compels the suppliers to focus on innovation to reduce the weight of their products while maintaining or increasing their acoustic performance.

There are mainly two strategies for the weight reduction of acoustic packages: development of new concepts or improvement of acoustic materials. Concerning the first, many innovations were patented during the last ten years [1]. These concepts are usually based on the multilayers systems (dash inner, floor insulator…) to absorb, to insulate the sound energy or to make use of the advantages of both of these two effects. To this end, porous materials such as foam or felt are always needed to assure the absorption function (for example a top absorbing layer) or insulation function (decoupling layer). From the product point of view, the total number of layers is limited to 4-5 layers due to process and cost constraints.

The second approach focuses on materials performance improvement, in that field the Design of Experiment (DoE) method is widely applied by both engineers and researchers. This method studies the materials produced by different input parameters (materials formulation, process). Then through statistical analysis, one tries to determine the influence of these input parameters on the acoustic performance of materials. Let us mention that the DoE method could be efficient when the input parameters are independent [2]. Otherwise, even if the number of input parameters is always limited by using only the most influential ones, a large number of samples is still necessary to ensure that the study is representative. Basically, this method may be very costly and time-consuming.

In recent years, the link between the microstructure of porous media (foams, fibrous materials, and also some granular porous samples) and its acoustical macro-behavior has been more and more studied [3]-[9]. These studies allow computing the acoustic properties of porous materials from their microstructural characteristics. Some of these studies could be used to define the optimal microstructure of porous materials reaching a targeted acoustic performance. Following this purpose, Perrot et *al.* studied the optimal microstructure of a porous material, represented by a hexagonal 2D porous structure, in order to obtain high absorption properties [9]. This is however quite correct for PUR foams whose microstructure could be better represented by other 3D geometrical models. Duval et *al.* used the method of Hoang and Perrot [7] to define the microstructure of PUR foam corresponding to targeted acoustic performance, but only a few numerical experiments were conducted [11].

Based on the micro-macro link studied by Hoang and Perrot for PUR foam [7], this work aims at determining the optimal cell morphology space of PUR foam reaching high acoustic performance. To this end, full numerical experiments were carried out, using a large range of input parameters to produce the response

surface representing the acoustic performance of PUR foam. The present paper is organized as follows: In Sec. 2, the approaches linking microstructure to the macroscopic acoustic properties of PUR foam are summarized. These approaches are then applied to define the optimal microstructure of PUR foam for insulation or absorption applications. The corresponding results will be presented respectively in Sec. 3 and Sec. 4. The end of this paper will be dedicated to a few concluding remarks (Sec. 5).

2. Approaches to link microstructure and acoustical macro-behavior

2.1 Equivalent fluid model for porous media

The fluid-saturated rigid-framed porous media can be represented by an equivalent fluid whose acoustic behavior can be determined using two frequency-dependent response functions, one characterizes the viscous effects and the other relates to the thermal effects [10].

There are several possible functions representing the viscous effect, let us mention here the dynamic tortuosity $\tilde{\alpha}(\omega)$, the dynamic viscous permeability $\tilde{k}(\omega)$ or the effective density $\tilde{\rho}(\omega)$, where ω is the angular frequency of air motion. These functions are linked by:

$$\tilde{\alpha}(\omega) = \tilde{\rho}(\omega) / \rho_0 , \quad [1]$$

$$\tilde{\alpha}(\omega) = \nu\phi / i\omega\tilde{k}(\omega) , \quad [2]$$

where ρ_0 and ν are respectively the density and the kinematic viscosity of air, ϕ is the porosity of porous material, i is a unit imaginary number.

Similarly, the various dynamic response functions characterizing the thermal dissipation of air in the pores are the normalized dynamic compressibility $\tilde{\beta}(\omega)$, the dynamic thermal permeability $\tilde{k}'(\omega)$ and the effective dynamic bulk modulus $\tilde{K}(\omega)$ of air in the pores. One of these functions can be found from the others by the following equations:

$$\tilde{\beta}(\omega) = K_a / \tilde{K}(\omega) , \quad [3]$$

$$\tilde{\beta}(\omega) = \gamma - (\gamma - 1) i\omega\tilde{k}'(\omega) / \nu'\phi , \quad [4]$$

where $K_a = \gamma P_0$ is the air adiabatic bulk modulus, P_0 is the atmospheric pressure, $\gamma = C_p / C_v$ is the specific heat ratio at constant temperature where C_p and C_v are the specific heat capacity at constant pressure and volume, $\nu' = \kappa / \rho_0 C_p$ where κ is the thermal conductivity of air.

The dynamic response functions mentioned above could be determined from the well-known semi-phenomenological models [12]-[15], in which the transport parameters of porous media are required. In the most complete model, these transport parameters are: porosity ϕ, static viscous permeability k_0, tortuosity α_∞, thermal characteristic length Λ', viscous characteristic length Λ, thermal permeability k_0', static tortuosity α_0 and thermal tortuosity α_0'. The static viscous permeability k_0 is related to the airflow resistivity σ of porous material via the dynamic viscosity of air $k_0 = \eta / \sigma$. The dynamic response functions can be represented in a general form, as below for the effective density and the effective bulk modulus:

$$\tilde{\rho}(\omega) = \rho_0 \alpha_\infty \left[1 + \frac{1}{i\varpi} f(\varpi) \right] , \quad [5]$$

$$\frac{1}{\tilde{K}(\omega)} = \frac{1}{K_a} \left\{ \gamma - (\gamma - 1) \left[1 + \frac{1}{i\varpi'} f'(\varpi') \right]^{-1} \right\} , \quad [6]$$

where f and f' are form functions defined by

$$\tilde{f}(\varpi) = 1 - P + P\sqrt{1 + \frac{M}{2P^2} i\varpi} , \quad [7]$$

$$\tilde{f}'(\varpi') = 1 - P' + P'\sqrt{1 + \frac{M'}{2P'^2} i\varpi'} , \quad [8]$$

and ϖ and ϖ' are dimensionless viscous and thermal angular frequencies given by the following expressions,

$$\varpi = \frac{\omega}{\nu} \frac{k_0 \alpha_\infty}{\phi} , \quad \varpi' = \frac{\omega}{\nu'} \frac{k_0'}{\phi} . \quad [9]$$

The quantities M, M', P and P' are dimensionless shape factors,

$$M = \frac{8 k_0 \alpha_\infty}{\Lambda^2 \phi} , \quad M' = \frac{8 k_0'}{\Lambda'^2 \phi} , \quad [10]$$

$$P = \frac{M}{4\left(\frac{\alpha_0}{\alpha_\infty} - 1 \right)} , \quad P' = \frac{M'}{4(\alpha_0' - 1)} . \quad [11]$$

The equivalent fluid models are classified depending on the number of required input transport parameters as follows:

- "Johnson-Champoux-Allard" [JCA] model: $M' = P = P' = 1$ (with the requirement that $k_0' \approx \phi\Lambda'^2/8$), the dynamic visco-inertial and thermal response functions depend on five parameters (ϕ, k_0, α_∞, Λ, Λ').
- "Johnson-Champoux-Allard-Lafarge" [JCAL] model: when the requirement $k_0' \approx \phi\Lambda'^2/8$ is not fulfilled, k_0' must be explicitly taken into account, then six parameters are necessary (ϕ, k_0, α_∞, Λ, Λ', k_0').

- "Johnson-Champoux-Allard-Pride-Lafarge" [JCAPL] model: A complete model relies on eight parameters (ϕ, k_0, α_∞, Λ, Λ', k_0', α_0, and α_0').

For the engineering application, the JCA model (sometimes called Allard model) is the most used model because the thermal permeability k_0' and the two tortuosities α_0 and α_0' are not usually measured and not much influencing parameters as compared to the other parameters. This model is combined with the Biot theory [16]-[17] to take into account the elastic properties of materials' frame, the modified model is called "Biot-Allard" model [10]. It is selected in this work to compute the macroscopic acoustic properties of foam.

2.2 Hybrid numerical approach

In order to define the micro-structural parameters of porous materials corresponding to their optimal acoustic performance, we need to know the relationship between the macroscopic acoustic properties (insulation or absorption) of the materials and their local geometry parameters. Due to the complexity of the real porous materials' microstructure and to the related physical problems, it is difficult to determine this micro-macro link through a complete analytical description. However, this could be studied by using numerical computation or experiments (see, for examples, Refs. [3]-[9].

From a numerical point of view, this multi-scale link is fully determined and validated for the PUR foam by Hoang and Perrot using the hybrid numerical approach; this method will be briefly recalled hereunder (for further details, see [7]).

The hybrid numerical method allows computing the response functions of porous materials for a full range of frequencies [6]. This method clearly offers more advantages as compared to the direct FEM dynamic simulation for which computation at each frequency is needed [4]. The latter leads to a more costly and time-consuming computation and thus could not be conveniently used for optimization purposes. The hybrid numerical approach is based on three steps:

- Determination of the representative elementary volume (VER) of porous material from the study of its local geometry which could be obtained by means of a few imaging techniques, such as optical or scanning electronic microscopy (2D) or even X-ray microtomography (3D). Particularly when the long-wavelengths acoustic waves' propagation hypothesis is fulfilled (this means that the wavelength is much larger than the microstructural characteristic size of porous materials), a scale separation is obtained. In this last condition, a PUC could be proposed to represent the porous materials' microstructure (See Refs. [18] and [19]).
- Next, the transport parameters within the porous material can be computed by resolving three asymptotic problems: k_0 and α_0 relate to the (incompressible) Stokes flow; Λ and α_∞ come from the solution of the potential flow and k_0' and α_0' are determined from the thermal conduction problem. The resolution of these three problems can be found by applying the homogenization method for periodic structure on the PUC defined in the first step as in Ref. [19].
- Once the transport parameters are obtained, the acoustic macro-parameters of the materials are computed from the equivalent fluid models recalled in the previous section.

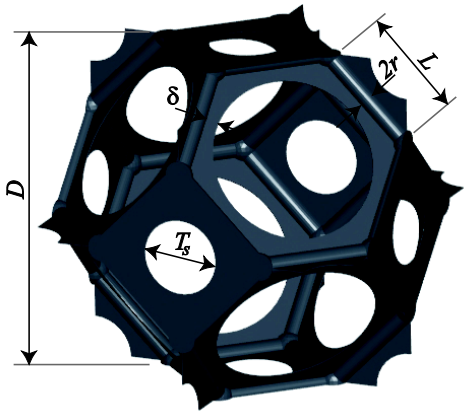

Figure 1: Tetrakaidecahedral PUC with solid films

Hoang and Perrot [7] used this numerical strategy to study the microstructure – acoustical macro-behavior relationship for PUR foams. First, a tetrakaidecahedral periodic unit-cell was proposed with ligaments of circular cross-section (Fig. 1, *L* and *2r* being respectively the ligament length and thickness). These ligaments are connected at their junction via a spherical node. At each squared or hexagonal face of the unit-cell, a very thin plate with round holes bridging together the ligaments is modeled to represent the foam membranes (or solid films) created during the foaming process. Here, the width δ of the membrane is the same in the squared face as in the hexagonal one. This value defines the closure rate of membrane of foam $\delta/\delta_{\max}$, where $\delta_{\max}$ is the width of the membrane on the squared face when this face is completely closed. Therefore, in this model; the closure rate of membranes varies from 0 to about 2 depending on the porosity of the foam. These two extreme values correspond respectively to fully reticulated and completely closed foam.

Next, basing on the proposed PUC, a methodology is proposed to compute the transport parameters of the

foam. This requires three input parameters: two non-acoustic parameters k_0 and ϕ and a microstructural size such as the ligament length L_m. The static permeability k_0 is related to the airflow resistivity σ via the dynamic viscosity of air as already mentioned. Knowing the transport parameters, the acoustical macro-parameters can be computed by means of equivalent fluid models.

The method proposed by Hoang and Perrot is well validated on several real polyurethane samples ([7], [20]). This will be the reference method used in the current paper to determine the optimal microstructure of PUR foam.

2.3 Semi-empirical model

With the same objective, Doutres and his collaborators investigated the links between the microstructure of PUR foams and its transport properties by using a semi-empirical method [5]. Several real PUR foam samples are studied which are fully reticulated (fully open pores) or partially reticulated (closed or partially closed pores). The microstructures of foams under their study present a large range of cell sizes and membrane content; these latter are the main micro-geometry foam's key parameters behind the ligament thickness t which is in most cases related to the ligament length L via the foam porosity ϕ for a given PUC.

For the partially reticulated foam, by also considering an isotropic tetrakaidecahedral periodic unit-cell with membranes, Doutres and his collaborators improved the existing scaling laws (Refs. [3],[10],[21]) by the 3-parameter semi-empirical model as named by the authors [22], to correlate the transport parameters with the microstructural properties of foams. It is worth to mention that a parameter which represents the open window content is defined: the reticulated rate R_w being the ratio of the number of open windows to the total number of windows of foam's microstructure. Thus the closed pore content equals to $(1-R_w)$ and this is physically equivalent to the closure rate of membrane defined in the work of Hoang and Perrot [7]. Among the different ligament cross-section shapes, from circular to triangular concave ones, taken into account by the authors, the triangular concave cross-section shape presented the best results. From an empirical point of view, when the porosity is fairly high this is reasonable because the concave triangle is the most similar shape compared to the real PUR foam cross-sections which are known as Plateau Borders. Consequently, in this section we recalled only the formulations proposed by Doutres et *al.* using the triangular concave cross-section shape hypothesis [22].

Inspired by the work of Perrot et *al.* [3] the two pure geometrical parameters, the porosity ϕ and the thermal characteristic length Λ', were determined by the geometric calculations based on the proposed periodic unit-cell:

$$\phi = 1 - \frac{\left(2\sqrt{3}-\pi\right)}{\sqrt{2}}\left(\frac{t}{L}\right)^2, \qquad [12]$$

$$\Lambda' = \frac{8L\sqrt{2}}{3}\frac{1-\dfrac{t^2\left(2\sqrt{3}-\pi\right)}{L^2\sqrt{2}}}{1+2\sqrt{3}-R_w\left(1+2\sqrt{3}-\dfrac{4\pi t}{L\sqrt{3}}\right)}. \qquad [13]$$

The other transport parameters are also proposed by adapting the existing scaling laws when the reticulated rate R_w is introduced to fit their values characterized from real foam samples (Refs. [10],[21]):

$$\sigma = 9\eta\left(\pi\frac{t}{L^2}\right)^2\left(\frac{1}{R_w}\right)^{1.1166}, \qquad [14]$$

$$\Lambda = \frac{\Lambda'}{1.55}\left(\frac{1}{R_w}\right)^{-0.6763}, \qquad [15]$$

$$\alpha_\infty = 1.05\left(\frac{1}{R_w}\right)^{0.3802}, \qquad [16]$$

A complete set of transport parameters necessary for the JCA model is therefore accessible from the micro-geometry parameters for the studied family of porous samples.

According to what can generally be observed on the microstructure of the studied real PUR foams, the latter formulations are not fully adequate when only the closed or opened windows are taken into account to represent the membrane content (as a definition of the reticulated rate R_w by Doutres et *al.*). In this way, the influences of partially closed membranes are not considered. The method of Doutres and his collaborators is however mostly validated on the real foam samples' absorption properties; this methodology is thus used later for comparison purposes.

On the other hand, it is relevant from the above formulations of Doutres and *al.* to use the same three input parameters as used by Hoang and Perrot [7]: porosity ϕ, airflow resistivity σ and a microstructural size such as the ligament length L. The ligament thickness t can be calculated from the porosity ϕ and the ligament length L by using Eq. [12]. Knowing ligament length and thickness, the reticulated rate R_w is computed from the airflow resistivity σ via Eq. [14]. Then all three required parameters (L, t, R_w) of the 3-parameter semi-empirical model are defined

allowing computation of the characteristic lengths Λ, Λ' and tortuosity α_∞ from Eqs. [14] to [16].

3. Decoupling foam

3.1 Mass/spring concept

In all of well-known automotive insulation solutions such as mass spring system or Light-Weight Concept (LWC: 3 layers, Absorber + Barrier + Decoupler), the foam layer in contact with the body in white is used as a decoupler [1]. This section will focus on this decoupling function optimization. For this purpose, a pure insulation "mass-spring" system is studied with a heavy layer (HL) on the top of decoupling foam (Fig. 2). The heavy layer is a high density impervious material representing the "mass" element; this layer is separated from the steel via the "spring" foam to form a double-wall system (Steel + Foam + Heavy layer). To estimate the performance of the insulator (Heavy layer + foam) independently from the steel, the Insertion Loss (IL) is proposed as the difference of transmission loss (TL) between the overall system with steel and the one without steel:

$$IL = TL_{Insulator+Steel} - TL_{Steel} \,. \qquad [17]$$

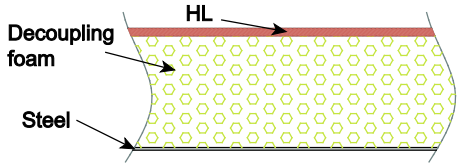

Figure 2: Classical spring foam + HL concept

Generally the Insertion Loss of such double-wall system increases at about 12 dB/octave up to the coincidence frequency when it works properly. This approximative linear increment leads this classic concept to be used efficiently in many cases to answer the insulation demand in vehicles.

3.2 Optimized microstructure of decoupling foam

This part is dedicated to defining the optimized microstructures of PUR foam corresponding to its best decoupling function. For this purpose a simple system is studied with heavy layer of 3.5 kg/m^2 on the top of 20mm soft PUR foam, this double layer is laid on a thin steel plate.

A first study was done by Duval and his collaborators to set the Biot-Allard parameters target setting for insulation problem [11]. The main objective of this work is to improve the Biot-Allard parameters of standard soft foam by changing only one parameter at a time and by computing the corresponding Transmission Loss with the FTMM (Finite Transfer Matrix Method) simulation [10],[23]. Then the microstructure of foam corresponding to improved parameters could be determined by using the hybrid numerical approach [7]. This method allows defining a better foam microstructure but this is not necessarily an optimal due to the low number of cases investigated.

For a real optimization, a full numerical experiment is needed in the current work. The hybrid numerical approach applied for foam by Hoang and Perrot is used, with three input parameters (Sec. 2.2): porosity ϕ, airflow resistivity σ and a microstructural size such as the ligament length L_m. The elastic parameters of PUR foam are however fixed: density $\rho = 55$ kg/m^3 ; Young's modulus $E = 15$ kPa.

Several parametric studies are then carried out for a large range of input parameters. For each triplet of input parameters, a set of transport parameters is defined corresponding to a unique microstructure of foam. The Insertion Loss of the HL − foam system is then computed by using FTMM simulation with a spatial windowing to take into account the finite size of sample [10],[24]. Because the simulated Insertion Loss is a frequency-dependence parameter, the Insertion Loss at 1000 Hz, named "IL_{1000Hz}", is proposed to approximately represent the insulation performance of the insulator from the IL curve.

Effect of cell size

Following this approach, the effect of cell size D is first studied. A large range of cell sizes is used which respects the pore sizes of common PUR foams. The input airflow resistivity σ increases from a low value of about 10 000 Nm^{-4}s to a sufficient high value beyond all foam's airflow resistivities proposed by Duval et *al*. [11]. The foam porosities ϕ are between 0.90 and 0.99. All parameters are rendered dimensionless via the cell-size D_{ref} which is defined as the cell size of a standard foam.

Fig. 3 illustrates the IL_{1000Hz} as a function of the dimensionless static permeability k_0/D_{ref}^2 (k_0 relates to σ through the dynamic viscosity of air, $k_0 = \eta/\sigma$) and the dimensionless cell size D/D_{ref} at a given porosity. Each point in Fig. 3(a-c) corresponds thus to a triplet of input parameters, from which a foam's microstructure together with a set of transport properties are determined. The acoustic performance such as IL_{1000Hz} is computed thanks to these transport parameters and presented by different colors in the figure. The non-physical input parameters are eliminated (purple color), that means these input parameters are not representative of any real foam microstructure. The different contours are also plotted so that every dot in a contour generates the same IL_{1000Hz} and all points inside this contour present a IL_{1000Hz} higher than the value shown on the contour.

Fig. 3 shows that the insulation level of foam depends clearly on the cell size, for example at ϕ =0.95,

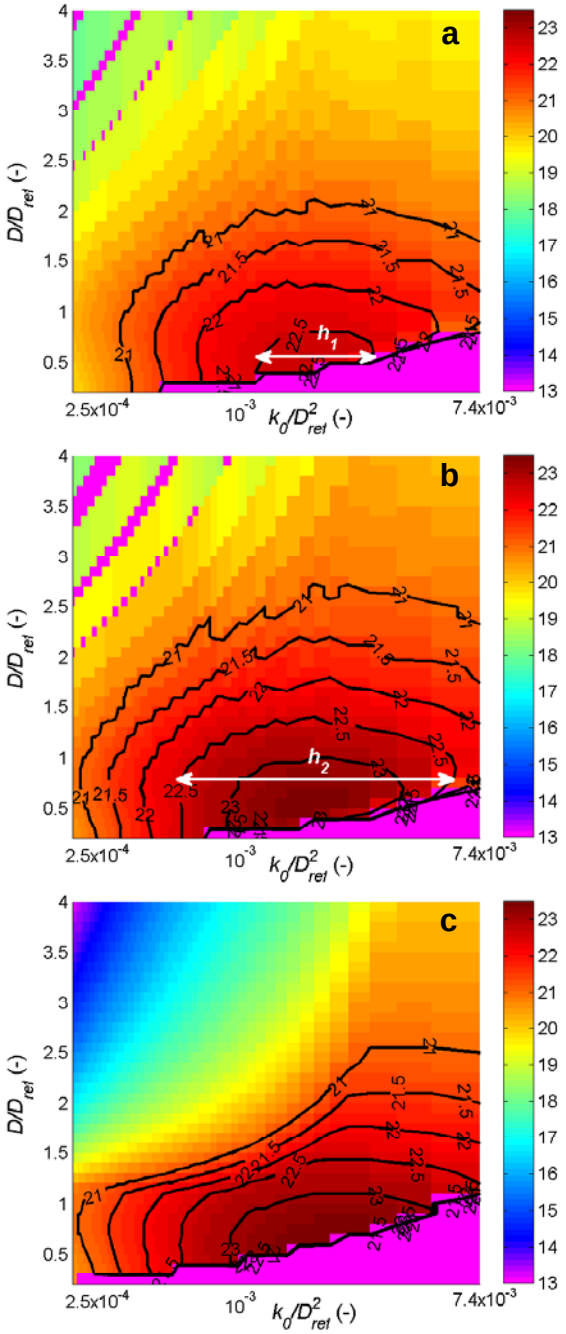

Figure 3: Insertion Loss IL_{1000Hz} (dB) response surfaces corresponding to various dimensionless cell sizes D/D_{ref} and dimensionless static permeabilities k_0/D_{ref}^2 at porosities 0.90 (a) and 0.95 (b-c). The 3-parameter semi-empirical model [5] is used in (c).

D/D_{ref} must be less than 2.5 to reach IL_{1000Hz} > 21 dB. In particular, the initial foam ($D/D_{ref} = 1$) could further be improved by decreasing the cell size down to the high performance area (better than 22.5-23 dB). Regarding porosity, we note that in the range between 0.90 and 0.99 the optimal area IL_{1000Hz} varies significantly. For example, at porosity 0.95 the high performance area is larger and about 0.5 dB higher compared to the porosity 0.90 corresponding area (Fig. 3(a-b), $h_2 > h_1$). Consequently it is important to take the influence of porosity into account in the foaming process.

It is also interesting to test the 3-parameter semi-empirical model of Doutres et *al.* for the numerical experiments. The result shown in Fig. 3c correlates quite well with the result using hybrid numerical approach (Fig. 3b) at the same porosity of 0.95, particularly at the high performance zone with IL_{1000Hz} better than 23 dB.

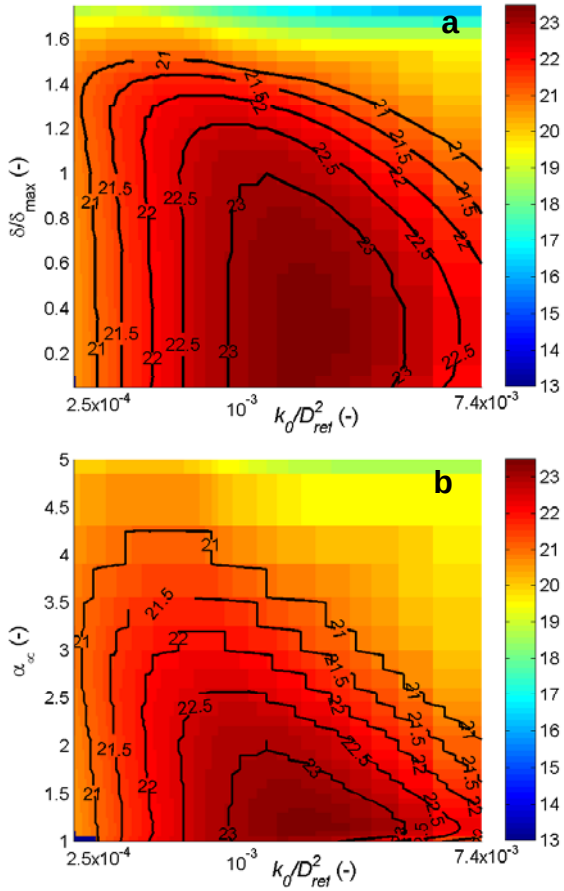

Figure 4: Insertion Loss IL_{1000Hz} (dB) response surfaces corresponding to various membrane closure rates δ/δ_{max} (a) or tortuosities α_∞ (b) and dimensionless static permeabilities k_0/D_{ref}^2 at porosity 0.95.

Effect of membrane closure rate

To investigate the influence of membrane content on the performance of the decoupling foam, the same strategy is used (this time) with the membrane closure rate δ/δ_{max} replacing the cell size *D* as the input parameter. The result illustrated on Fig. 4a indicates that δ/δ_{max} must be inferior or equal to 1 to be in the optimal area with IL_{1000Hz} better than 23 dB.

Using the proposed model, this means that it is preferable not to have any closed window on the real foam sample. It must be emphasized that the tortuosity strongly depends on the membrane closure rate: this parameter increases while the membrane content becomes larger. That explains why tortuosity α_∞ should not be greater than two to be in the high performance area, as illustrated on Fig. 4b.

4. Absorbing foam

4.1 Light-weight concept

The classical "mass-spring" system presents a very poor absorption near to zero caused by the lack of absorbing material on the top of this pure insulation concept. In order to reduce the mass, during the last decade, many multilayer systems were proposed mixing both insulation and absorption [1].

An example of a Light-Weight Concept, with three layers, is illustrated on Fig. 5, where the top layer is an absorbing material, the bottom one is a decoupling (spring) layer and the barrier is a heavy layer.

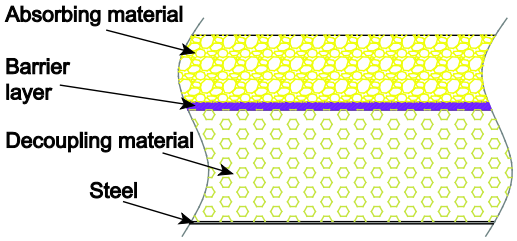

Figure 5: Light-Weight Concept with 3 layers

4.2 Optimized microstructure of absorbing foam

The objective of this part will be dedicated to define the optimized microstructure of the absorbing foam which could be used as the top absorbing layer in a system such as LWC. For the latter, a 10 mm absorbing foam is studied, with density $\rho = 90$ kg/m^3 and Young's modulus $E = 500$ kPa.

The same strategy as the one used in the study of decoupling foam (previous section) is adopted while varying different input parameters [7]. For each three input parameters e.g. [ϕ, σ and D or δ/δ_{max}], a set of transport parameters is computed. Then the sound absorption coefficient α of 10 mm foam is simulated by using the TMM in which the Biot-Allard model is used, with a diffuse field excitation for which the integration of the plane wave for different angles from 0 to 90° is performed.

Once again, a criterion is necessary to estimate the absorption performance from the frequency-dependence absorption curve. The first one that we used is the sound absorption average (*SAA*) defined by the ASTM standard which is a "single number rating of sound absorption coefficient of a material for the twelve one-third octave bands from 200 through 2500Hz inclusive" [25]. The *SAA* number thus covers the low and middle frequency ranges: $SAA = \frac{1}{12}\sum_{f=200Hz}^{f=2500Hz} \alpha(f)$ where $\alpha(f)$ is the sound absorption coefficient at frequency f.

In order to focus also on high frequency, we define another criterion named *SC* (sound absorption class) which takes the average value of sound absorption coefficient in a given one-third octave band from 2000Hz to 6300Hz included: $SC = \frac{1}{6}\sum_{f=2000Hz}^{f=6300Hz} \alpha(f)$.

Effect of cell size

The same cell size range as used in the study of the decoupling foam is proposed because these are the pore sizes of common PUR (decoupling or absorbing) foam. The input airflow resistivity σ increases from a low value of about 10 000 Nm^{-4}s to very high value to ensure that this range covers the potential performance area on the response surface. A very

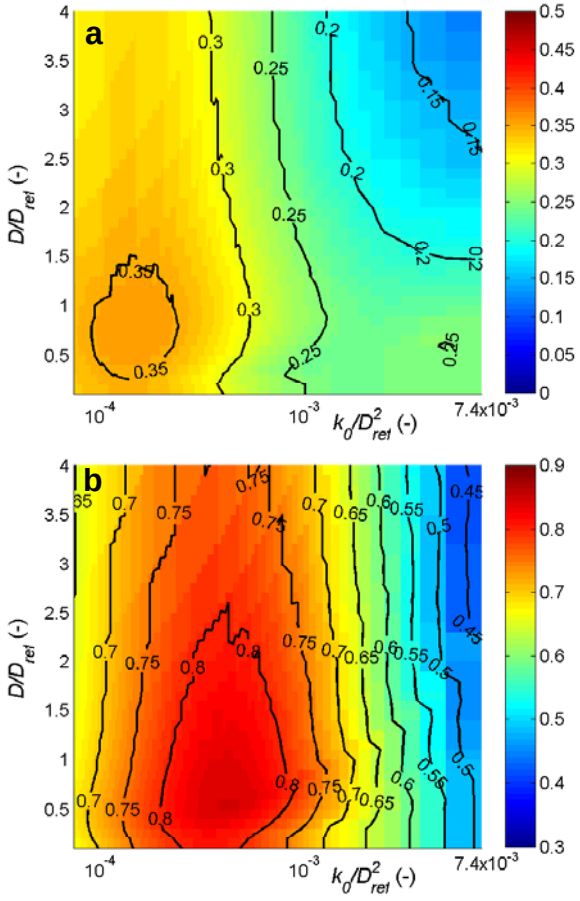

Figure 6: *SAA* number (a) and *SC* class (b) response surfaces at porosity 0.95 depending on dimensionless cell size D/D_{ref} and dimensionless static permeability k_0/D_{ref}^2.

high number of computations is thus necessary (at a given porosity, about 20 000 computations were made during less than 2 days) and the response surface is too dense to be visibly illustrated on this paper. That is why we present only the area around the high performance domain.

The *SAA* number displayed in Fig. 6a shows that the sound absorption coefficient of a 10 mm PUR foam sample is small in the low and middle frequency ranges (α_{max}<0.5). The optimized possible area corresponds to a rather low static permeability k_0 (high airflow resistivity σ) while the cell size D/D_{ref} is less then 1.5.

Moreover, Fig. 6b in terms of *SC* class gives a higher absorption (α_{max}>0.8) because in the *SC* class the absorption coefficient at high frequency is taken into account. We can also conclude that the cell size *D* effect is less significant in the absorption than the static permeability k_0 (or airflow resistivity σ): we can have a rather high performance if *D* reaches the maximum size, however the performance is strongly decreased if k_0 is too low or too high.

Effect of membrane closure rate

Finally, the membrane content effect is investigated with various closure rates δ/δ_{max} (from fully open pore to extremely closed pore). The result illustrated on Fig. 7 for both *SAA* and *SC* classe shows once again a very significant effect of static permeability k_0, versus the effect of membrane (whose effect is still important but less than the effect of k_0). Generally, the permeability k_0 depends on the microstructure of foam with a combination of several parameters (cell size, window size…) but not in a linear way. It is empirically demonstrated from the Eq. [14] that k_0 (related to σ by air viscosity) depends on all of three microstructure parameters: ligament length *L*, thickness *t* and membrane content.

5. Conclusions and future works

In this paper, the optimized microstructures of PUR foams are identified reaching different acoustic targets. By using the micro-macro numerical approach of Hoang and Perrot, the micro-geometry properties of foam, such as cell size or membrane content, vary, together with a large range of porosity and airflow resistivity, to produce the acoustic response surfaces. This strategy is first applied for decoupling foam in any insulating system. It is found that both cell size and membrane closure rate are important and greatly affect the functionality of insulating foam, in particular the membrane's closure rate is preferable at a value lesser or equal to 1. Following the same strategy, absorbing foam such as

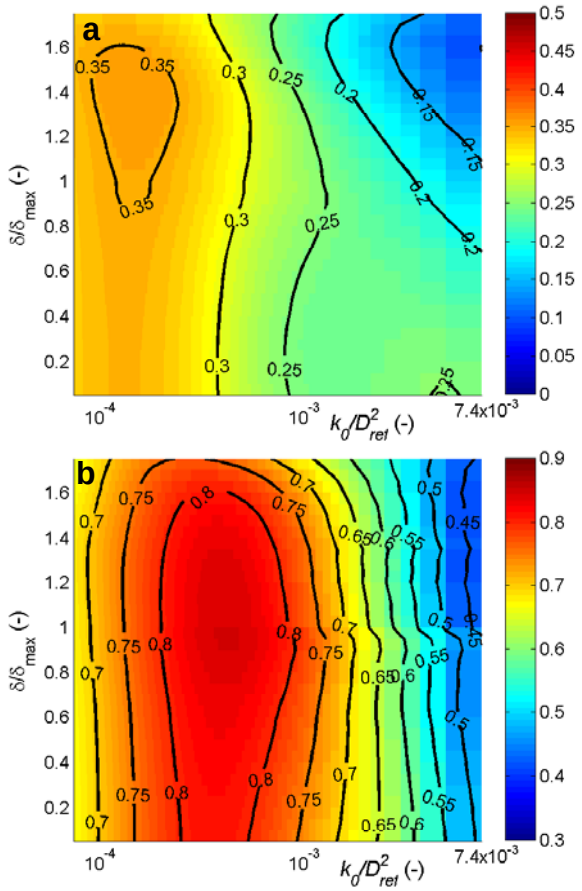

Figure 7: *SAA* number (a) and *SC* class (b) response surfaces at porosity 0.95 depending on membrane closure rate δ/δ_{max} and dimensionless static permeability k_0/D^2_{ref}.

the top layer in a Light-Weight Concept is then studied. The results present a high dependence of sound absorption on the airflow resistivity (permeability) of foam for both low and high frequency behavior.

The trend for optimized microstructures defined in this work is very useful to guide foam production where the cell size or membrane content could be controlled by different methods (foam formulation, cell openers…). This gives a high potential for not only better acoustic performance system but also for weight reduction. The optimization methodology used in this work could be applied to other porous materials (fibers, felt, foam with inclusions…) when their micro-macro links are known.

6. Acknowledgement

The authors would to thank Arnaud Duval for the fruitful discussions in this study, Carl François from *Acoustic TechCenter - Faurecia* for reviewing and Marie-Hélène Alexandre for assistance in improving the English quality of this paper.

7. References

[1] A. Duval, J.-F. Rondeau, L. Dejaeger, F. Lhuillier and J. Monet-Descombey: "*Generalized Light-Weight Concepts: A New Insulator 3D Optimization Procedure*", SAE Conference, p. 12., Grand Rapids (MI), 2013.

[2] L. Bischoff, C. Morgenstern, W. Berhard, A. Zopp, S. Schreck: "*Replacement of damping pads by using soft visco-elastic foam while maintaining high insulation properties*", Internoise, p. 14., New York, 2012.

[3] C. Perrot, R. Panneton, and X. Olny: "*Periodic unit cell reconstruction of porous media: Application to an open cell aluminum foam*", J. Appl. Phys. 101, 113538, 2007.

[4] S. Gasser, F. Paun and Y. Bréchet: "*Absorptive properties of* rigid *porous media: Application to face centered cubic sphere packing*", J. Acoust. Soc. Am. 117(4), 2090-2099, 2005.

[5] O. Doutres, N. Atalla, and K. Dong: "*Effect on the microstructure closed pore content on the acoustic behavior of polyurethane foams*", J. Appl. Phys. 110, 064901, 2011.

[6] C. Perrot, F. Chevillotte, M. T. Hoang, G. Bonnet, F.-X. Bécot, L. Gautron, and A. Duval: " *Microstructure, transport, and acoustic properties of open-cell foam samples: Experiments and three-dimensional numerical simulations* ", J. Appl. Phys. 111, 014911, 2012.

[7] M. T. Hoang and C. Perrot: "*Solid films and transports in cellular foams*", J. Appl. Phys. 112, 054911, 2012.

[8] K. Gao, J.A.W. van Dommelen, P. Göransson, M.G.D. Geers: "*Computational homogenization of sound propagation in a deformable porous material including microscopic viscous thermal effects*", J. Sound Vib., 365, 119-133, 2016.

[9] C. Perrot, F. Chevillotte, and R. Panneton, "*Bottom-up approach for microstructure optimization of sound absorbing materials*", J. Acoust. Soc. Am. 124, 940, 2008.

[10] J. F. Allard and N. Atalla: "*Propagation of Sound in Porous Media: modeling sound absorbing materials*", 2nd Ed., Wiley, Chichester, 2009.

[11] A. Duval, M. T. Hoang, C. Perrot, V. Marcel, G. Bonnet: "*Chemistry-process morphology control of porous microstructures: a bottom-up acoustic optimization approach*", SIA-SFA Conference: Light-weighting and acoustical materials in vehicles, p. 8., Compiègne, France, 2013.

[12] Y. Champoux and J. F. Allard: "*Dynamic tortuosity and bulk modulus in air-saturated porous media*", J. Appl. Phys. 70, 1975-1979, 1991.

[13] D. Lafarge: "*Propagation du son dans les matériaux poreux à structure rigide saturés par un fluide viscothermique*", Ph. D. Thesis, Université du Maine, 1993; translation in English: "*Sound propagation in rigid porous media saturated by a viscothermal fluid*".

[14] D. Lafarge, P. Lemarinier, J. F. Allard and V. Tarnow: "*Dynamic compressibility of air in porous structures at audible frequencies*", J. Acoust. Soc. Am. 102 (4), 1995-2006, 1997.

[15] S. R. Pride, F. D. Morgan and A. F. Gangi: "*Drag forces of porous media acoustics*", Physical Review B 47 (9), 4964-4975, 1993.

[16] M. A. Biot, "*Theory of propagation of elastic waves in a fluid-filled-saturated porous solid - I. Low-frequency range*", J. Acoust. Soc. Am. 28(2), 168-178, 1956.

[17] M. A. Biot, "*Theory of propagation of elastic waves in a fluid-filled-saturated porous solid - II. Higher frequency range*", J. Acoust. Soc. Am. 28(2), 179-191, 1956.

[18] J.-L. Auriault: "*Heterogeneous medium. Is an equivalent macroscopic description possible*", Int. J. Eng. Sci. 29, 785, 1991.

[19] J.-L. Auriault, C. Boutin and C. Geindreau: "*Homogenization of coupled phenomena in heterogeneous media*", Wiley-ISTE, 2009.

[20] M. T. Hoang and C. Perrot: "*Identifying local characteristic lengths governing sound wave properties in solid foams*", J. Appl. Phys. 113, 084905, 2013.

[21] E. Lind-Nordgren and P. Göransson: "*Optimising open porous foam for acoustical and vibrational performance*", J. Sound Vibrat. 329(7), 753-767, 2010.

[22] O. Doutres, M. Ouisse, N. Atalla, and M. Ichchou: "*Impact of the irregular microgeometry of polyurethane foam on the macroscopic acoustic behavior predicted by a unit-cell model*", J. Acoust. Soc. Am. 136(4), 1666-1681, 2014.

[23] B. Brouard, D. Lafarge, J.-F. Allard: "*A general method of modelling sound propagation in layered media*", J. Sound Vib., 183, 129-42, 1995.

[24] M. Villot and C. Guigou-Carter, "*Using spatial windowing to take the finite size of plane structures into account in sound transmission,*" Proceedings of the NOVEM 2005, p. 8., Saint Raphaël, France, 2005.

[25] ASTM International, "*Standard test method for sound absorption and sound absorption coefficient by the reverberation room method*", C 423 – 02, 2002.

8. Glossary

ABA: Absorber/Barrier/Absorber

DoE: Design of Experiment

FEM: Finite Element Method

FTMM: Finite Transfer Matrix Method

IL: Insertion loss

LWC: Light-Weight Concept

PUR: Polyurethane

TL: Transmission loss

OEM: Original Equipment Manufacturer